Original research article

Oregano (*Origanum vulgare L.*) essential oil provides anti-inflammatory activity and facilitates wound healing in a human keratinocytes cell model

Rosanna Avola[a,b], Giuseppe Granata[b], Corrada Geraci[b*], Edoardo Napoli[b], Adriana Carol Eleonora Graziano[a], Venera Cardile[a*]

[a]Department of Biomedical and Biotechnological Sciences – Section of Physiology, University of Catania, Via Santa Sofia, 97 – 95123 Catania, Italy.

[b]Institute of Biomolecular Chemistry, National Research Council (C.N.R.), Via Gaifami, 18 - 95026 Catania, Italy.

*Corresponding authors:

V. Cardile; PhD; telephone: +39 095 4781318; email: cardile@unict.it; ORCID: 0000-0001-9902-3736;

C. Geraci; Dr; telephone: +39 0957338318; email: corrada.geraci@icb.cnr.it

Words total number: 7803 (Abstract: 200; Introduction: 500; Discussion: 1011; Conclusion: 113

Tables number: 3

Figures number: 8

ABSTRACT

Skin acts as a protective barrier between the body and the external environment. Skin wounds are a common inflammatory disorder for the solution of which plants and essential oils have been applied as a medical option for centuries. *Origanum vulgare* essential oil (OEO) is largely used in folk medicine, but its molecular mechanisms of action are not fully known. In this study, we evaluated the anti-inflammatory/antioxidant activity as well as wound healing capacity of a well-characterized OEO on human keratinocytes NCTC 2544 treated with interferon-gamma (IFN-γ) and histamine (H) or subjected to a scratch test. The expression of pro-inflammatory mediators such as ROS, inter cellular adhesion molecule ICAM-1, inducibile nitric oxide synthase iNOS, and ciclooxygenase COX-2 were verified. The DNA damage was shown by the formation of 8-oxo-7,8-dihydro-2'-deoxyguanosine (8-OHdG) and activation of proliferating cell nuclear antigen (PCNA). Moreover, the abnormal modification of extracellular matrix components (ECM) was examined by determining matrix metalloproteinase (MMP)-1, and -12. Compared to untreated control, OEO showed efficacy in supporting and enhancing the cell motility. In IFN-γ and H treated cells, OEO displayed a significant reduction of ROS, ICAM-1, iNOS, COX-2, 8-OHdg, MMP-1 and MMP12.. OEO proved useful to treat inflammation and support cell motility during wound healing.

Keywords: oregano; OEO; *in vitro* experiments; keratinocyte; healing; skin protective activity.

1. Introduction

Skin epidermis is a stratified squamous epithelium that provides a waterproof barrier and creates the skin tone. Keratinocytes as expressed in a ~95% are the main constituent cells intrinsically involved in the physiological maintenance of the structural and physical integrity of the skin. Furthermore, they are primary sensors of stressful conditions and play a relevant role in the skin response to a variety of agents including infectious microorganisms, toxic chemical compounds, physical injury and skin wounds (Russo et al., 2019). Currently, the wounds represent an important threat to global public health with a high social impact and a general decrease in the quality of life (Sen et al., 2009). Over recent decades, the mechanisms of wound repair have been studied extensively (Shaw and Martin, 2016) allowing to understand the role of keratinocytes in the beginning of the migration and proliferation from the wound margins (Margadant et al., 2009). In this field, many researchers have

focused their attention on the use of plants with pharmaceutical properties (Calixto, 2005). Furthermore, plants secondary metabolites essential oils are extensively used in aromatherapy and various traditional medicinal systems. Many of essential oils possess different pharmacological

properties deriving from the content of various bioactive compounds, some of which have potent anti-inflammatory effect. Origanum vulgare is a pervasive aromatic plant of the Lamiaceae family typical of Mediterranean flora that has been commonly used not only for medical purposes (Chun et al., 2005; Wojdylo et al., 2007; Ocana-Fuentes et al., 2010), but also in food, agricultural, veterinary, and pest control (Sahina et al., 2004; Granata et al., 2018). Moreover, the use of oregano essential oil (OEO) provides an interesting perspective in the prevention of neurodegenerative disorders (Loizzo et al.,

2009). These promising activities seem to be derived by the synergism of some major and minor components (Schillaci et al., 2013). However, studies on the effects of OEO in human skin cells are very few and, to the best of our knowledge, simply one study has reported the biological

activity of OEO in human dermal fibroblasts (Han et al., 2017). The aim of this research was to describe the biological effects of OEO in the restoring of physiological cell homeostasis during wound and inflammation phenomena. To accomplish this, human keratinocyte cell line NCTC 2544 was used as an inflammatory in vitro model obtained by interferon-gamma (IFN-γ) and histamine (H) stimulation or as a wound model attained by scratching the confluent monolayer of keratinocytes.

IFN-γ is an essential cytokine in amplifying inflammatory reactions because it stimulates the synthesis of chemokines that activate and attract inflammatory cells. Histamine is released from keratinocytes in

the early stage of inflammation of the skin and participates in the control of the inflammatory response by acting on lymphocytes, monocytes and leucocytes. Histamine binds to cell surface receptors coupled to G-proteins and induces various intracellular signalling pathways. These histamine receptor-mediated signals regulate cytokine or chemokine gene expression in target cells (Cardile et al., 2010a). The scratch-wound assay is a simple, reproducible assay commonly used to measure basic cell migration parameters such as speed, persistence, and polarity. Cells are grown to confluence and a thin "wound" introduced by scratching with a pipette tip. Cells at the wound edge polarize and migrate into the

wound space (Cory, 2011). Inflammation and wound healing implicate increase of reactive oxygen species (ROS) and reactive nitric species (RNS) and always damage to DNA (Heck et al., 1992).

To prove the biological activities of OEO, the expression of pro- inflammatory mediators such as inter-cellular adhesion molecule-1 (ICAM-1), inducible nitric oxide synthase (iNOS), and cyclooxygenase-

2 (COX-2) were determined. The DNA damage was verified by the formation of 8-oxo-7,8-dihydro-20-deoxyguanosine (8-OHdG)) and activation of the nuclear protein proliferating cell nuclear antigen (PCNA) (Moon et al., 2008). Moreover, the over-production of inflammatory cytokines and wounds trigger an abnormal modification of extracellular matrix components (ECM) through the alteration of matrix metalloproteinase (MMPs), with substrate specificities, secreted by keratinocytes

and dermal fibroblasts in response to multiple stimuli. Thus, in this work, we detected the role of collagenase-1 (MMP-1), that degrades basement membrane collagens, and elastase (MMP-12), that destroys primarily elastin.

2. **Materials and Methods**

2.1.Characterization of OEO

The OEO (provided by Esperis S.p.A., Milan, Italy) was characterized by gas chromatography (GC) and gas chromatography-mass spectrometry (GC–MS). As previously reported in (Granata et al., 2018), GC analyses were run on a Shimadzu gas chromatograph, Model 17-A equipped with a flame ionization detector (FID), and with operating software Class VP Chromatography Date System version 4.3 (Shimadzu, Milan, Italy). Analytical conditions: SPB-5 capillary column (15 m □

0.10 mm x 0.15 μm; Supelco, Milan, Italy); helium as carrier gas (1 mL/min); injection in split mode (1:200); injected volume 1 μL (4% essential oil/CH2Cl2 v/v); injector and detector temperatures 250 and 280 □C, respectively; linear velocity in column 19 cm/s. The oven temperature was held at 60 □C for 1 min, then programmed from 60 to 280 □C at 10 □C/min, then 280 □C for 1 min. Percentages of compounds were determined from their peak areas in the GC-FID profiles.

GC–MS was carried out in fast mode on a Shimadzu (Kyoto, Japan) GC–MS model GCMSQP5050A, with the same column and the same operating conditions used for analytical GC-FID, operating software GC-MS solution version 1.02 (Shimadzu, Milan, Italy). Ionization voltage was 70 eV, electron multiplier 900 V and ion source temperature 180 □C. Mass spectral data were acquired in scan mode in the m/z range 40–400. The

same oil solutions (1 μL) were injected in split mode (1:96).

2.2 *Identification of components of OEO*

The identification of essential oils components was carried out based on their GC retention index (relative to C9-C20 n-alkanes on the SPB-5 column), computer matching of spectral MS data with those from NIST MS libraries, the comparison of the fragmentation patterns with those reported in the literature (Adams, 2012) and, whenever possible, co-injections with authentic samples.

2.3 DPPH assay

The radical scavenging activity of OEO was assessed by diphenyl picrylhydrazyl (DPPH) assay [17]. Briefly, 20 μL of different concentrations of the essential oil in methanol were mixed with 2 mL of a 0.1 mM DPPH solution in methanol to obtain mixtures containing 0-400 μg/mL of OEO, respectively. The mixtures were stirred at 25 °C in the dark for 30 min. The absorbance at λ= 515 nm was recorded on an UV-VIS spectrophotometer (8453 UV–Visible spectrophotometer; Agilent Technologies, Santa Clara, CA). Methanol was used as a negative control, while BHT at concentration of 0-11.2 μg/mL was used as a positive control. The results of radical scavenging activity (RSA%) were obtained using the following formula:

$$\text{RSA}\ (\%) = \frac{A_0 - A_s}{A_0} \times 100$$

where A_0 and A_s are the absorbance values of negative control and samples, respectively.

The SC_{50} values were calculated by regression analysis ($R^2 > 0.99$) of RSA (%) versus of OEO (or BHT) concentration of each solution tested. The measurements were carried out in triplicate and the SC_{50} values were expressed as mean ± standard deviation.

2.4. Determination of total phenols content (TPC)

TPC in OEO was determined according to Folin-Ciocalteu assay with minor modifications. Specifically, 10 µL of diluted OEO (1 mg/mL in methanol) were mixed with 500 µL of 1 N Folin-Ciocalteu reagent, followed by the addition of 1 mL of water and 1 mL of Na_2CO_3 (1.9 M). Finally, the mixture was diluted to 10 mL final volume with water and kept for 2 hours at 25 °C in the dark. After incubation, the absorbance was measured at λ= 750 nm. A sample consisting of water and reagents was used as a blank. Gallic acid was used as a reference standard and TPC value (GAE/g of OEO) was estimated by comparison with a calibration curve (R^2 = 0.998) obtained plotting the absorbance at λ= 750 nm versus gallic acid concentration (20-100 µg/mL). Each experiment was performed in triplicate and the results as GAE value was expressed as mean ± standard deviation.

2.5. Cell culture and treatments

The normal human keratinocyte cell line NCTC 2544 (obtained by Interlab Cell Line Collection Genoa, Italy) were grown in Minimum Essential Medium (MEM, Sigma-Aldrich, Milan, Italy), containing 10% fetal bovine serum (FBS), 1% of streptomycin, 1% of penicillin and incubated in controlled conditions at 37 °C in a humidified, 95% air 5% CO_2 atmosphere. The culture medium was changed every 2–3 days. For experiments, 24 hours before the cells were trypsinized, counted, and plated in 96 (1.5×10^4), 24 (5×10^4), 6-well (3.0×10^5) plates or T-25 flask. Twenty-four hours after, the culture medium was discarded, and cells were washed with phosphate-buffered saline (PBS). Experimental keratinocytes were stimulated or not (untreated controls) with 200 U mL^{-1} of IFN-γ and 10^{-4} M of H, used to reproduce the mechanisms involved in the pathogenesis of inflammatory processes [41] in the presence or absence of different concentrations of OEO (5, 10,

25, 50, and 75 μg/mL for MTT assay and 25 μg/mL for other experiments). Commercially available indomethacin was used as a reference anti-inflammatory drug at 10 μM. After 72 hours, each sample was tested for the experiments described below.

2.6. Cell viability

OEO toxicity was assessed using the mitochondrial-respiration- dependent 3-(4,5-dimethylthiazol-2-yl)-2,5-diphenyltetrazolium (MTT) reduction method (Cardile et al., 2018). NCTC 2544 cells line were plated in 96 multi-wells and incubated with different concentrations of OEO for 24, 48 and 72 h at 37 □C in 5% CO2. After treatment, 20 μL of MTT (Sigma-Aldrich, Milan, Italy) in PBS at final concentration of 5 μg/mL were added. Afterwards 3 h, PBS was removed and the formazan crystals formed were solubilized with 100 μL of dimethylsulphoxide (DMSO). The absorbance of each well was measured by a microplate spectrophotometer reader (Titertek Multiskan, DAS, Milan, Italy). The optical density of formazan formed in control cells was taken as 100% viability and the data were averaged (three experiments in triplicate) and represented as percentage of viability with respect to untreated controls.

2.7. Determination of ROS

Antioxidant activity in cells was evaluated in NCTC 2544 cells line measuring the oxidation of 20,70-dichlorodihydrofluorescein diacetate (H2-DCFDA) (Sigma-Aldrich, Milan, Italy). H2-DCFDA diffuses through the cell membrane and is enzymatically hydrolyzed by intracellular esterase to the non-fluorescent H2-DCF. Intracellular ROS are able to oxidize H2-DCFDA to the fluorescent 20,70-dichlorofluorescein (DCF), whose intensity of fluorescence is directly proportional to the levels of intracellular ROS. According to the method described by Cardile et al. (2010b), cells (1.5 □104 cells/well) were cultivated in a 96-well plate and incubated in at 37 □C in 5% CO2. Twenty-four hours after, the culture medium was discarded and the wells were washed with PBS. The cells were treated in triplicates with 100 μL of H2-DCFDA (5 mM), and kept in incubation for 10 min (5%

CO2, 37 □C) and then washed in PBS. Next, 200 μL of OEO (25 μg/mL) solution were added. After 72 h the fluorescence was measured at excitation/emission wavelengths of λ ¼ 480/535 nm using a Hitachi F-2000 spectrofluorimeter (Hitachi, Tokyo, Japan). Values (three experiments in triplicate) were expressed as relative fluorescence units normalized versus the level of ROS in the control cells.

2.8. Determination of 8-hydroxy-2'-deoxyguanosine (8-OHdG)

The amount of DNA damaged was analyzed by the quantification of 8-OHdG production. NCTC2544 cells (5 x 10^4/well) were seeded on 24-well plates and treated with IFN-γ + H and OEO (25 μg/mL) or indomethacin. After 24 hours, the cells were fixed with 4% paraformaldehyde in PBS at 4 °C for 2 hours. Next, the cells were incubated with 0.05 N HCl for 5 min on ice, washed with PBS and incubated with 300 μL of RNAse (100 μg/mL dissolved in 150 mM NaCl and 15 mM sodium citrate) for 1 hour at 37 °C. Subsequently, NCTC 2544 were dehydrated in a graded alcohol series (35, 50, and 75% ethanol), washed in PBS and incubated with 300 μL of 0.15 M NaOH in 70% ethanol for 4 min to denature DNA *in situ*. The alkaline solution was neutralized by 70% ethanol containing 4% formaldehyde. After, the cells were treated with 50%, 35% ethanol, and PBS. Next, 300 μL of proteinase K (5 μg/mL in 20 mM Tris and 1 mM EDTA, pH 7.5) were added to the cells and incubated for 10 min at 37 °C. To prevent non-specific binding the samples were blocked with 5% BSA for 1 hour at room temperature. The cells were subsequently incubated overnight at 4 °C with a primary antibody direct against anti-8-OHdG (sc-393870; Santa Cruz Biotechnology, Santa Cruz, CA, USA; 1:200 dilution). The following day, cells were washed with PBS and incubated for 1 hour at room temperature with a fluorescein isothiocyanate conjugated goat anti-mouse (12-506, FITC; Millipore, Milan, Italy; 1:400 dilution) antibody. After washed with PBS the level of binding was measured at excitation/emission wavelengths of λ= 488/519 nm using a Hitachi F-2000 spectrofluorimeter (Hitachi, Tokyo, Japan). The cell density was assessed by the incubation of all experimental cultures with 4′,6-Diamidino-2-phenylindole dihydrochloride (DAPI, Invitrogen,

Milan, Italy; 1:10000 dilution) for 10 min at room temperature and the measure of fluorescence intensity (λ = 346/460 nm). Values (three experiments in triplicate) were expressed as fold change versus untreated control.

2.9. Wound healing scratch assay

To study OEO action during wound healing, the human keratinocytes cell line NCTC 2544 was functionalized to realize an artificial wound in a confluent monolayer of cells. NCTC 2544 were seeded a density of 1×10^4 cells/well into 6-well plates, and then cultured for 48 hours, at which time the cells had reached ~80% confluence. Subsequent to the cell monolayer being scratched with a sterile 200 μL pipette tip, the cells were treated with OEO and then incubated for a further 24, 48 and 72 hours to allow time for migration into the cell-free area.

2.10. Reverse transcriptase-polymerase chain reaction (RT-PCR)

RT-PCR assay was performed and analyzed as previously described in Avola et al. [20]. Total RNA from NCTC 2544 treated and not was isolated using 1 ml Qiazol Reagent (Qiagen, Milan, Italy), 0.2 mL chloroform, and 0.5 mL isopropanol. Pellet was washed with 75% ethanol, dried with air, and re-suspended in RNAse-free water. Total RNA was purified using the Qiagen RNeasy Mini Kit (Qiagen, Milan, Italy). The complementary DNA (cDNA) were synthesized from the total RNA samples by using the QuantiTect Reverse Transcription Kit (Qiagen, Milan, Italy) according to the manufacturer's protocol. Aliquots of cDNA were amplified using specific primers sequences reported in **Table 2**.

2.11. Gene expression quantification

RT-PCR analysis was performed by Rotor-gene Q (Qiagen, Milan, Italy) [21]. Specifically, cDNA template (100 ng/reaction) was added to the reaction mix containing 1x Rotor-Gene SYBR Green PCR Master Mix (Qiagen, Milan, Italy), 1 μM of each primer (forward and reverse) (**Table 2**) and RNase-free water to a final reaction volume of 25 μL. RT-PCR was performed using the

following program: initial activation step 95 °C 10 min, denaturation 95 °C 10 s, annealing 60 °C 30 s, extension 72 °C 30 s (40 cycles), final extension 72 °C 10 min. RT-PCR was followed by melting curve analysis to confirm PCR specificity. Each reaction was repeated three times and threshold cycle average was used for data analysis by Rotor-gene Q software. Target genes were normalized against GAPDH. Amplification products were separated by electrophoresis in a 2% agarose gel in 0.045 M Tris–borate/1mM EDTA (TBE) buffer. Each amplification was carried out in duplicates in four different experiments. The $2^{-\Delta\Delta CT}$ method was used to calculate the difference in CT value between the OEO-treated samples and untreated controls. Results were then normalized to an endogenous reference gene (GAPDH) whose expression is constant in all groups.

$$\Delta\Delta CT = (CT_{Target} - CT_{Reference\ gene})_{treated} - (CT_{Target} - CT_{Reference\ gene})_{untreated}$$

The results were reported as fold change of IFN-γ + H-treated cells vs. untreated control.

2.12. Western blot analysis

The protein expression of inflammatory biomarkers was evaluated by Western blot. Keratinocytes NCTC 2544 were lysed with buffer M-PER Mammalian Protein Extraction Reagent (Pierce, Fisher Scientific, Milan, Italy) and vortexed for 30 min on ice. The insoluble debris was removed by centrifugation at 15,000 × g for 15 min at 4 °C. The proteins quantification was performed by the bicinchoninic acid assay (BCA assay; Pierce, Fisher Scientific, Milan, Italy). The proteins in equal amount (40 μg) were separated by 4–12% bolt gel (Invitrogen, Milan, Italy) and electrophoretically transferred to nitrocellulose membranes (Invitrogen, Milan, Italy) in a wet system (Invitrogen, Milan, Italy). The transfer of proteins was verified by staining the nitrocellulose membranes with Ponceau S. Membranes were blocked in 10 mL of iBind flex solution (Thermo Fisher Scientific, Milan, Italy) for 30 min at room temperature. Primary antibodies, reported in **Table 3**, and the appropriate HRP-conjugated secondary antibody (goat anti-rabbit, 1:5000 dilution; goat

anti-mouse, 1:1000 dilution, both Santa Cruz Biotechnology, DBA, Milan, Italy) were diluted in iBind flex solution and incubated on the membranes by iBind™ Flex Western System (Thermo Fisher Scientific, Milan, Italy) overnight at room temperature. Blots were rinsed in distillate water and the specific antibodies were detected with chemiluminescent solution (Pierce, Fisher Scientific, Milan, Italy) and visualized by Uvitec Alliance LD9 gel imaging system (Uvitec, Cambridge, UK). Bands were measured densitometrically and their relative density was calculated based on the density of the α-tubulin bands in each sample. Values of arbitrary densitometric units (A.D.U.) (three experiments in triplicate) corresponding to signal intensity were expressed as fold of change with respect to untreated control.

2.13. Statistical analysis

The assays were performed at minimum three times in triplicate and all data were expressed as the mean ± SD (Standard Deviation). Student's t-test for paired and variance analysis (ANOVA) for unpaired data were used. All statistical analyses were made using the statistical software package SYSTAT, version 11 (Systat Inc., Evanston IL, USA). A value of $p < 0.05$ was considered to indicate a statistically significant difference.

3. Results

3.1 Chemical composition of OEO

The complete characterization of OEO by GC and GC-MS is reported in Table 1. The mayor component is carvacrol (35.95±0.22%) followed by thymol (25.2±0.27%), p-cymene (21.54 ±0.35%), and linaool (4.26 ±0.05%). All other compounds were below 4%. In terms of chemical families, oxygenated monoterpenes are the main class (60.97%) followed by monoterpene hydrocarbons (25.80%) and sesquiterpenes (14.23%) (Licata et al., 2015; Napoli and Ruberto, 2012).

3.2. Determination of total phenolic content (TPC)

The total phenolic content (TPC) assay showed that OEO is a rich in phenolic compounds. In fact, TPC value, expressed as mg of gallic acid equivalent (GAE) per g of OEO, was 214 □6. TPC and SC50 values are indicative of the good antioxidant properties of OEO.

3.3. Cell viability

To determinate whether OEO is able to influence cellular viability and to establish the work concentration to use, NCTC 2544 were exposed to different doses of OEO (3, 5, 7.5, 10, 12, 25, and 50 μg/mL). After 24, 48 and 72 h of treatment, MTT of experimental cultures was performed. The safety profile of OEO was calculated by comparison of cell viability respect to untreated/control cells. The results of the MTT assay (Fig. 1) showed that OEO has no effect on cell viability, because the treatment of cells at different doses did not reduce the ability of NCTC 2544 to metabolize tetrazolium salts up to 25 μg/mL. A slight non-significant decrease in cell viability was present at 50 μg/mL. Thus, we decided to use the concentration of 25 μg/mL for subsequent experiments.

3.4. Determination of reactive oxygen species (ROS)

ROS have been reported to be involved in cell damage induced by inflammation. To characterize the level of oxidative stress and to assess the changes in intracellular ROS levels caused by IFN-γ and H without or with 25 μg/mL of OEO, confluent NCTC 2544 cells were treated with H2DCFDA 72 h after the stimulation. Indomethacin (10 μM) was used as a reference anti-inflammatory drug. The fluorescence signal, as an indicator of intracellular oxidants, was measured after 10 min and compared to that of the control cells. H2DCFDA can be taken up into cells and then oxidized by ROS to its fluorescent derivative DCFDA. As expected, we found that, with respect to the control cells, the treatment with IFN-γ and H induced a high fluorescent signal, indicating a massive production of ROS. The cultures treated with OEO showed a significant lower level of ROS (Fig. 2).

3.5. Determination of 8-OHdG

Inflammation is recognized as a potential mechanism of injury able to produce oxidative stress and subsequently cells and DNA architecture damages. To verify whether IFN-γ and H-induced oxidative stress was linked to DNA damage, we performed the quantification of 8-OHdG. As compared with controls, 8-OHdG generated in cells stimulated with IFN-γ and H alone was very high. When the NCTC 2544 cells were stimulated with IFN-γ and H in presence of OEO (25 µg/mL), we found a reduction of 8-OHdG content (Fig. 3). It suggests that OEO prevents in keratinocytes, at least partly, the formation of endogenous DNA adducts induced by IFN-γ and H stimulation. This protective effect of OEO was greater than that of indomethacin.

3.6. Tissue remodeling activity

To detect the effect OEO on the promotion of basic cell functions such as the cell proliferation, we have performed in vitro the scratch wound healing assay. OEO showed efficacy in supporting and enhancing the physiological cell motility after the monolayer lesion without changes in cell morphology. As observed in Fig. 4A and B, a more pronounced improvement of artificial lesion was observed with OEO treatment (25 µg/mL) 0–72 h after injury. The re-populated area between the wound margins was monitored at different time intervals (0,24, 48, and 72 h) after the lesion. Cell migration was evaluated by measuring the cell-free surface at the beginning of the experiment (T0) and the surface covered by cells at each time interval by using Image J software (National Institute of Health, USA). Results are expressed as migration rate in each condition.

3.7. Anti-inflammatory and antioxidant activity of OEO

To study the anti-inflammatory effects of OEO in our experimental model of inflammation, we have evaluated in IFN-γ and H-stimulated NCTC 2544 cells the amount of mRNA and proteins of ICAM-1, iNOS and COX-2 by reverse transcriptase-polymerase chain reaction (RT-PCR) and Western blot, respectively. The data reported in Fig. 5A and B showed that the levels of three major inflammation biomarkers were significantly increased following IFN-γ and H treatment for 72 h.

However, the addition of OEO (25 μg/mL) for 72 h significantly reduced the IFN-γ and H induced mRNA of ICAM-1, iNOS, and COX-2, respectively. We also investigated if OEO affects the expression of these same biomarkers at the protein level. As shown in Fig. 5B, OEO significantly decreased the protein levels of ICAM-1, iNOS, and COX-2. Moreover, we have also compared the effect of treatment with OEO respect to the application ofindomethacin (10 μM), and, as described in Fig. 5, OEO inhibited ICAM-1, iNOS, and COX-2 to a higher degree. The analyzed biomarkers never reached the basal level of unstimulated cells, but their significant down-regulation suggested OEO as an inducer or supporter of cell homeostasis restoration during inflammatory event.

3.8. Determination of MMP-1 and -12

To study the effects of OEO on the degradation of ECM components induced by IFN-γ and H, we tested the profile of MMP-1 and -12, at the gene and protein level by RT-PCR and Western blot, respectively, using the total amount of RNA and proteins isolated from experimental cells (Figs. 6 and 7). As showed in Fig. 6A and B, compared with untreated controls, keratinocytes exposed to IFN-γ and H demonstrated a significant increase in the MMP-1 levels, suggesting that IFN-γ and H treatment is involved in the stimulation of MMPs gene expression. The addition of OEO (25 μg/mL) in IFN-γ and H treated NCTC 2544 cells reduced the MMP-1 levels. Indomethacin (10 μM) significantly inhibited the up- regulation of MMP-1 stimulated by IFN-γ and H, but compared to OEO reduced to a lower degree. These data suggest the involvement of OEO in the reduction of ECM disruption by the inhibition of breakdown of matrix collagens, proteoglycans and glycoproteins. Furthermore, Western blot analysis and RT-PCR of keratinocytes stimulated with IFN-γ and H showed high levels of MMP-12 (a skin elastase) implicated in the metabolism of elastic fibers and associated with the decrease in skin elasticity and consequent formation of wrinkles in various types of tissues during acute or chronic inflammation disease. When in the cultures exposed to IFN-γ and H was added OEO or indomethacin, a general reduction of MMP-12 mRNA and protein content was

determined (Fig. 7A and B). Compared to indomethacin, OEO (25 μg/mL) inhibited the MMP-12 expression to a higher grade.

3.9. Determination of PCNA

To determine a molecular link between the support of inflammation resolution and the improvement of wound healing, we have decided to evaluate by immunoblot, under inflammatory condition, the expression protein level of PCNA, a marker of proliferating cells. As expected, the analysis revealed that PCNA-positive immunoblot was observed in the control cells (Fig. 8). The NCTC 2544 inflammation by IFN-γ and H for 72 h increased PCNA expression, while the amount of PCNA signal was significantly decreased by treatment with OEO (25 μg/mL) (Fig. 8). These results indicated that OEO acts as both an inducer of cell proliferation and a supporter of cellular regeneration by PCNA modulation.

4. **Discussion**

The OEO sample possessed a typical Sicilian oregano profile (Licata et al., 2015) composed of low molecular weight volatile components, such as monoterpene and sesquiterpenes known for the wide range of biological and pharmacological properties like antioxidant, immunomodulatory, anti-cancer, anti-hepatotoxic, and anti-microbial activity (Chun et al., 2005; Oca~ na-Fuentes et al., 2010). The monoterpenes account for about 61% of the OEO and are endowed as powerful inhibitor of the pro-inflammatory cytokines IL-1β, IL-6, and TNFα (Bukovska et al., 2007; Oca~ na-Fuentes et al., 2010). These properties make these compounds strong candidates for the development of biotechnological products for the management of skin damage, tissue repair, and wound healing. As previously described by Graziano et al. (2012), the epidermis possesses two types of proliferating keratinocytes actively involved in the dynamic and well-ordered biological process that allow to achieve and/or restore the skin integrity. Wound healing is a complex process that involves the control of the homeostasis, inflammation, proliferation, formation, and remodeling of new tissue (Harper et

al., 2014). Thus, the aim of our research was to evaluate the cicatrizing and anti-inflammatory activity of OEO using as an in vitro cell model human keratinocytes NCTC 2544. Our study confirmed a noticeable antioxidant/anti-inflammatory activity as well as tissue remodeling and wound healing capacity of OEO containing a pool of compounds such as phenolic compounds, carvacrol and thymol, and other minor components, including monoterpene hydrocarbons, such as p-cymene and γ-terpinene (Licata et al., 2015). In particular, OEO has a significant anti-inflammatory property, acting as a potent inhibitor against pro-inflammatory damage from IFN-γ and H in human keratinocytes. The treatment with OEO was, in fact, able to diminish the release of a variety of pro-inflammatory mediators like iNOS, ICAM-1, and COX-2. Moreover, OEO treatment reduced the ROS development, reduced 8-OHdG formation, and maintained the PCNA expression without influencing cell viability. Probably, human keratinocytes stimulated by IFN-γ and H produce iNOS that is able to interact with COX-2 causing S-nitrosylation of COX-2 cysteines, which enhances COX-2 catalytic activity (Albouchi et al., 2018). As reported in Graziano et al. (2018), increased expression of pro-inflammatory cytokines has been associated with increased expression of ICAM-1, a cell surface glycoprotein belonging to immunoglobulin (IgG) super family, that participates in inflammatory reactions by interacting with lymphocyte function associated antigen-1 (LFA-1) and macrophage-1 antigen (Mac-1) expressed on lymphocytes and macrophages, respectively. The interaction of ICAM-1 with LFA-1 results in the adhesion of cells, and consequent activation of signal transduction mechanisms, which facilitate the infiltration of leukocytes into the tissues, lymphocyte proliferation, cytotoxic T cell function and T cell mediated B cell activation. There is extensive experimental evidence that oxidative damage permanently occurs to lipids of cellular membranes, proteins, and DNA. 8-OHdG is the most abundant type of radical-induced oxidative DNA lesions with a formation mechanism strictly due to the predominant reaction mediated by singlet molecular oxygen (Droge, 2002). Specifically, ROS can attack base and sugar moieties in DNA yielding a variety of lesions

such as apurinic and apyrimidinic sites, DNA strand breaks, or oxidized bases. In nuclear and mitochondrial DNA, 8-hydroxy-20-deoxyguanosine (8-OHdG) or 8-oxo-7,8-dihydro-20-deoxyguanosine (8-OXOdG) is one of the predominant forms of free radical-induced oxidative lesions, and has therefore been widely used as a biomarker for oxidative stress (Kasai, 1997). In our study, 8-OHdG content significantly increased after treatment with IFN-γ and H, which is consistent with the changes in the ROS levels. ROS levels are decreased by the contemporary administration of OEO contributing to the decrease of 8-OHdG induced by IFN-γ and H stimulation. Increased ROS levels are also associated with increases in mitogen-activated protein kinases (MAPK) activation and the expression of PCNA and cyclin D1, two of the most important modulators directly involved in cell proliferation and cell cycle progression. PCNA, a cofactor of DNA polymerase δ is present in reduced amounts in resting cells and is synthesized at higher rate during the S phase of growing cells. PCNA is a homotrimeric protein that forms a sliding clamp around DNA and acts as a processivity factor for the replicative polymerase. PCNA also interacts with many other proteins such as translation synthesis polymerases, which plays a crucial role in targeting them to the damage site and stimulating their enzymatic activity. Hence, PCNA is an essential protein that functions in DNA replication, repair, recombination, damage tolerance, and cell cycle control. Its deregulation is an indication of cellular damage (Avola et al., 2019). Moreover, we have detected the decreasing of MMP-1 and MMP-12 levels induced by inflammatory IFN-γ and H. These results supported the hypothesis that OEO has a role in preserving the ECM remodeling and tissue healing. Upon injury of the skin, the migration of keratinocytes is essential for wound re-epithelialization and re-establishment of skin remodeling (Sivamani et al., 2007). In this context, our results show an improving of NCTC 2544 cell proliferation induced by OEO. It is well documented that MMPs are essential to the remodeling of the extracellularmatrix. While their upregulation facilitates aging and cancer, they have a crucial role in epidermal differentiation and the prevention of wound scars. The

pharmaceutical industry is active in identifying products that inhibit MMPs to prevent or treat the inflammatory states linked to aging or cancer conditions and stimulate MMPs to prevent epidermal hyperproliferative diseases and wound scars (Philips et al., 2011). Overproduction of tissue remodeling enzymes including MMP-1 is important causes of inflammatory pathologies associated with irreversible tissue destruction. Specifically during the wound, MMP-1 cleaves fibrillar type I collagen and is needed to initiate keratinocyte migration (Pilcher et al., 1997). MMP-12 is the most effective MMP against elastin that suffers posttranslational modification by keratinocytes and fibroblast. In our experimental conditions, MMP-12 was secreted in response to keratinocytes inflammation playing a crucial role in the development of elastosis produced by the collection of dystrophic elastic material in the dermis. In addition, MMP-12 is also responsible for the activation of other pro-MMPs, such as pro-MMP-1, MMP-2, MMP-3, and MMP-9 (Pittayapruek et al., 2016). The ability of OEO to control these parameters may be attributed to the radical scavenging properties of monoterpene fraction. The GC and GC-MS analyses of OEO showed the carvacrol is the most abundant phenolic compound belonging to the class of oxygenated monoterpenes (35.95 □0.22%). It is important to note that carvacrol appears to be responsible for OEO activities owing to its antioxidant and tissue remodeling properties. Regarding hazard classification and labelling, European Chemical Agency (ECHA) reports that for OEO there is no harmonized classification and there are no notified hazards by manufacturers, importers or downstream users even if a majority of data submitters agrees this substance is skin sensitizing. Skin reactions are the most common types of adverse reaction to essential oils, but these are individual reactions, do not happen the first time of use, are dependent on sex (women more sensitive than men) and above all concentrations. Tisserand and Young (2014) indicated that when using OEO there is a moderate risk of skin sensitization, and they recommended a dermal maximum of 1.1%, so the concentration (25 μg/mL) used in our experimental conditions would be harmless even on hypersensitive skin. Regarding absorption, distribution, metabolism and

excretion (ADME), no specific studies with OEO were provided, so the ADME of the individual constituents is therefore considered. In mammals, carvacrol and thymol are rapidly absorbed from the gastrointestinal tract, mainly conjugated with sulfate and glucuronic acid and excreted in the urine. Besides carvacrol and thymol, the compounds identified in the essential oil are monoterpenes (see Table 1). The most abundant of these terpenoids is p-cymene, a precursor of carvacrol and thymol. In general, monoterpenes are expected to be absorbed from the gastro-intestinal tract and oxidized to polar oxygenated metabolites (by the cytochrome P450 enzymes, alcohol dehydrogenase and aldehyde dehydrogenases). The resulting hydroxylated metabolites and carboxylic acids may be excreted in conjugated form or undergo further oxidation, yielding more polar metabolites that are also excreted in conjugated form in the urine. Oxidation of the double bond leads to epoxide intermediates that are rapidly transformed either by hydrolysis to yield diols, or by conjugation with glutathione. The enzymes involved in the biotransformation pathways of these compounds are present in all the animal species including humans. Moreover, some studies have observed no adverse effects up to 200 mg/kg bw per day (Bampidis et al., 2019).

5. Conclusion

This study reports for the first time the results in vitro of a commercial oregano essential oil with known and standardized content of bioactive molecules and suggests some metabolic partners involved in the performance of its biological activities. OEO has proven useful in reducing some parameters involved in inflammation and in supporting cell motility during wound healing. Additional research steps are needed to verify the OEO use for in vivo treatment of skin repair and/or inflammatory diseases.

Declaration of competing interest

The authors declare that they have no known competing financial interests or personal relationships that could have appeared to influence the work reported in this paper.

CRediT authorship contribution statement

Rosanna Avola: Conceptualization, Investigation, Methodology, Writing - original draft. Giuseppe Granata: Investigation, Methodology, Data curation, Validation.

Corrada Geraci: Conceptualization, Data curation, Funding acquisition, Writing - review & editing.

Edoardo Napoli: Investigation, Methodology, Data curation, Validation.

Adriana Carol Eleonora Graziano: Investigation, Methodology.

Venera Cardile: Conceptualization, Supervision, Funding acquisition, Writing -

review & editing.

Acknowledgments

The authors wish to thank Dr. Angela Patti, (Institute of Biomolecular Chemistry, National Research Council, C.N.R., Catania, Italy) for her scientific encouragement. This work was supported by a grant from University of Catania, Ricerca Finanziata Ateneo, Cod. 21040104 and by Project « Chemical enabling technologies for health and environment» in the framework FSO PO 2014–2020 Regione Sicilia (11/2017, CUP: G67B17000150009).

References

Adams, R.P., 2012. In: Identification of Essential Oil Components by Gas Chromatographic/quadrupole Mass Spectrometry, (4th Ed.), Carol Stream (IL). Allured Publ. Corp.

Albouchi, F., Avola, R., Dico, G.M.L., Calabrese, V., Graziano, A.C.E., Abderrabba, M., Cardile, V., 2018. Melaleuca styphelioides Sm. polyphenols modulate interferon gamma/histamine-induced inflammation in human NCTC 2544 keratinocytes. Molecules 23, E2526. https://doi.org/10.3390/molecules23102526 pii.

Avola, R., Graziano, A.C.E., Pannuzzo, G., Cardile, V., 2017. Human mesenchymal stem cells from adipose tissue differentiated into neuronal or glial phenotype express different aquaporins. Mol. Neurobiol. 54, 8308–8320. https://doi.org/10.1007/s12035-016-0312-6.

Avola, R., Graziano, A.C.E., Pannuzzo, G., Albouchi, F., Cardile, V., 2018. New insights on Parkinson's disease from differentiation of SH-SY5Y into dopaminergic neurons: an involvement of aquaporin4 and 9. Mol. Cell. Neurosci. 88, 212–221. https://doi.org/10.1016/j.mcn.2018.02.006.

Avola, R., Graziano, A.C.E., Pannuzzo, G., Bonina, F., Cardile, V., 2019. Hydroxytyrosol from olive fruits prevents blue-light-induced damage in human keratinocytes and fibroblasts. J. Cell. Physiol. 234, 9065–9076. https://doi.org/10.1002/jcp.27584.

Bampidis, V., Azimonti, G., Bastos, M.L., Christensen, H., Kouba, M., Durjava, M.K., Lopez-Alonso, M., Lopez Puente, S., Marcon, F., Mayo, B., Pechova, A., Petkova, M., Ramos, F., Sanz, Y., Villa, R.E., Woutersen, R., Brantom, P., Chesson, A., Westendorf, J., Gregoretti, L., Manini, P., Dusemund, B., 2019. Safety and efficacy of an essential oil from Origanum vulgare ssp. hirtum (Link) Ietsw for all animal species. EFSA J. 17, 1–14. https://doi.org/10.2903/j.efsa.2019.5909.

Bukovska, A., Cikos, S., Juhas, S., Il'kova, G., Rehak, P., Koppel, J., 2007. Effects of a combination of thyme and oregano essential oils on TNBS-induced colitis in mice. Mediat. Inflamm. 23296. https://doi.org/10.1155/2007/23296, 2007.

Calixto, J.B., 2005. Twenty-five years of research on medicinal plants in Latin America: a personal view. J. Ethnopharmacol. 100, 131–134. https://doi.org/10.1016/j. jep.2005.06.004.

Cardile, V., Libra, M., Caggia, S., Frasca, G., Umezawa, K., Stivala, F., Mazzarino, M.C., Bevelacqua, Y., Coco, M., Malaponte, G., 2010a. Dehydroxymethylepoxyquinomicin, a novel nuclear factor-jB inhibitor, prevents inflammatory injury induced by interferon-c and histamine in NCTC 2544 keratinocytes. Clin. Exp. Pharmacol. Physiol. 37, 679–683. https://doi.org/10.1111/j.1440-1681.2010.05375.x.

Cardile, V., Frasca, G., Rizza, L., Rapisarda, P., Bonina, F., 2010b. Antiinflammatory effects of a red orange, extract in human keratinocytes treated with interferon-gamma and histamine. Phytother Res. 24, 414–418. https://doi.org/10.1002/ ptr.2973.

Cardile, V., Avola, R., Graziano, A.C.E., Piovano, M., Russo, A., 2018. Cytotoxicity of demalonyl thyrsiflorin A, a semisynthetic labdane-derived diterpenoid, to melanoma cells. Toxicol. Vitro 47, 274–280. https://doi.org/10.1016/j.tiv.2017.12.012.

Chun, S., Vattem, D.A., Lin, Y.T., Shetty, K., 2005. Phenolic antioxidants from clonal oregano (Origanum vulgare) with antimicrobial activity against Helicobacter pylori. Process Biochem. 40, 809–816. https://doi.org/10.1016/j.procbio.2004.02.018.

Cory, G., 2011. Scratch-wound assay. Methods Mol. Biol. 769, 25–30. https://doi.org/ 10.1007/978-1-61779-207-6_2.

Droge, W., 2002. Free radicals in the physiological control of cell function. Physiol. Rev.

82, 47–95. https://doi.org/10.1152/physrev.00018.2001.

Foti, M.C., Daquino, C., Geraci, C., 2004. Electron-transfer reaction of cinnamic acids and their methyl esters with the DPPH radical in alcoholic solutions. J. Org. Chem. 69, 2309–2314. https://doi.org/10.1021/jo035758q.

Granata, G., Stracquadanio, S., Leonardi, M., Napoli, E., Consoli, G.M.L., Cafiso, V., Stefani, S., Geraci, C., 2018. Essential oils encapsulated in polymer-based nanocapsules as potential candidates for application in food preservation. Food Chem. 269, 286–292. https://doi.org/10.1016/j.foodchem.2018.06.140.

Graziano, A.C., Cardile, V., Crascì, L., Caggia, S., Dugo, P., Bonina, F., Panico, A., 2012. Protective effects of an extract from Citrus bergamia against inflammatory injury in interferon-gamma and histamine exposed human keratinocytes. Life Sci. 90, 968–974. https://doi.org/10.1016/j.lfs.2012.04.043.

Graziano, A.C.E., Pannuzzo, G., Salemi, E., Santagati, A., Avola, R., Longo, E., Cardile, V., 2018. Synthesis, characterization, molecular modeling, and biological evaluation of thieno-pyrimidinone methanesulphonamide thio-derivatives as nonsteroidal anti-inflammatory agents. Clin. Exp. Pharmacol. Physiol. 45, 952–960. https://doi.org/ 10.1111/1440-1681.12962.

Han, X., Rodriguez, D., Parker, T.L., 2017. Biological activities of frankincense essential oil in human dermal fibroblasts. Biochim. Open 4, 31–35. https://doi.org/10.1016/j. biopen.2017.01.003.

Harper, D., Young, A., Mc Naught, C.E., 2014. The Physiology of Wound Healing. Surgery (Oxford), pp. 445–450. https://doi.org/10.1016/j.mpsur.2014.06.010.

Heck, D.E., Laskin, D.L., Gardner, C.R., Laskin, J.D., 1992. Epidermal growth factor suppresses nitric oxide and hydrogen peroxide production by keratinocytes.

Potential role for nitric oxide in the regulation of wound healing. J. Biol. Chem. 267, 21277–21280. PMID: 1383221.

Kasai, H., 1997. Analysis of a form of oxidative DNA damage, 8-hydroxy-20

-

deoxyguanosine, as a marker of cellular oxidative stress during carcinogenesis. Mutat. Res. 387, 147–163. https://doi.org/10.1016/s1383-5742(97)00035-5.

Licata, M., Tuttolomondo, T., Dugo, G., Ruberto, G., Leto, C., Napoli, E.M., Rando, R., Virga, G., Leone, R., La Bella, S., 2015. Study of quantitative and qualitative variations in essential oils of Sicilian oregano biotypes. J. Essent. Oil Res. 27, 293–306. https://doi.org/10.1080/10412905.2015.1045088.

Loizzo, M.R., Menichini, F., Conforti, F., Tundis, R., Bonesi, M., Saab, A.M., Statti, G.A., Cindio, B.D., Houghton, P.J., 2009. Chemical analysis, antioxidant, antiinflammatory and anticholinesterase activities of Origanum ehrenbergii Boiss and and Origanum syriacum L. essential oils. Food Chem. 117, 174–180. https://doi. org/10.1016/j.foodchem.2009.03.095.

Maksimovic, Z., Stojanovic, D., So□ staric, I., Dajic, Z., Ristic, M., 2008. Short communication composition and radical-scavenging activity of thymus glabrescens willd. (Lamiaceae) essential oil. J. Sci. Food Agric. 88, 2036–2041. https://doi.org/ 10.1002/jsfa.3311.

Margadant, C., Raymond, K., Kreft, M., Sachs, N., Janssen, H., Sonnenberg, A., 2009. Integrin α3β1 inhibits directional migration and wound re-epithelialization in the skin. J. Cell Sci. 122, 278–288. https://doi.org/10.1242/jcs.029108.

Moon, H.J., Lee, S.R., Shim, N., Jeong, S., Stonik, S.H., Rasskazov, V.A., Zvyagintseva, T., Lee, Y.H., 2008. Fucoidan inhibits UVB-induced MMP-1 expression in human skin

fibroblasts. Biol. Pharm. Bull. 31, 284–289. https://doi.org/10.1248/bpb.31.284.

Napoli, E.M., Ruberto, G., 2012. Sicilian aromatic plants: from traditional heritage to a new agro-industrial exploitation. In: Kralis, J.F. (Ed.), Spices: Types, Uses and Health Benefits. Nova Science Publishers, New York, pp. 1–56.

Ocana-Fuentes, A., Arranz-Gutierrez, E., Senorans, J., Reglero, G., 2010. Supercritical fluid extraction of oregano (Origanum vulgare) essentials oils: anti-inflammatory properties based on cytokine response on THP-1 macrophages. Food Chem. Toxicol. 48, 1568–1575. https://doi.org/10.1016/j.fct.2010.03.026.

Philips, N., Auler, S., Hugo, R., Gonzalez, S., 2011. Beneficial regulation of matrix metalloproteinases for skin health. Enzym. Res. https://doi.org/10.4061/2011/427285.

Pilcher, B.K., Dumin, J.A., Sudbeck, B.D., Krane, S.M., Welgus, H.G., Parks, W.C., 1997. The activity of collagenase-1 is required for keratinocyte migration on a type I collagen matrix. J. Cell Biol. 137, 1445–1457. https://doi.org/10.1083/jcb.137.6.1445.

Pittayapruek, P., Meephansan, J., Prapapan, O., Komine, M., Ohtsuki, M., 2016. Role of matrix metalloproteinases in photoaging and photocarcinogenesis. Int. J. Mol. Sci. 17, E868. https://doi.org/10.3390/ijms17060868.

Russo, A., Cardile, V., Graziano, A.C.E., Avola, R., Montenegro, I., Cuellar, M., Villena, J., Madrid, A., 2019. Antigrowth activity and induction of apoptosis in human melanoma cells by Drymis winteri forst extract and its active components. Chem. Biol. Interact. 305, 79–85. https://doi.org/10.1016/j.cbi.2019.03.029.

Sahina, F., Güllüce, M., Daferera, D., S€ okmen, A., S€ okmen, M., Polissiou, M., Agar, G., €

Ozer, H., 2004. Biological activities of the essential oils and methanol extract of Origanum vulgare ssp. vulgare in the Eastern Anatolia region of Turkey. Food Contr. 549–557. https://doi.org/10.1016/j.foodcont.2003.08.009.

Schillaci, D., Napoli, E.M., Cusimano, M.G., Vitale, M., Ruberto, G., 2013. Origanum vulgare subsp. hirtum essential oil prevented biofilm formation and showed antibacterial activity against planktonic and sessile bacterial cells. J. Food Protect. 76, 1747–1752. https://doi.org/10.4315/0362-028X.JFP-13-001.

Sen, C.K., Gordillo, G.M., Roy, S., Kirsner, R., Lambert, L., Hunt, T.K., Gottrup, F., Gurtner, G.C., Longaker, M.T., 2009. Human skin wounds: a major and snowballing threat to public health and the economy. Wound Repair Regen. 17, 763–771. https://doi.org/10.1111/j.1524-475X.2009.00543.x.

Shaw, T.J., Martin, P., 2016. Wound repair: a showcase for cell plasticity and migration. Curr. Opin. Cell Biol. 42, 29–37. https://doi.org/10.1016/j.ceb.2016.04.

Sivamani, R.K., Garcia, M.S., Isseroff, R.R., 2007. Wound re-epithelialization: modulating keratinocyte migration in wound healing. Dermatology 12, 2849–2868. https://doi.org/10.2741/2277.

Tisserand, R., Young, R., 2014. Essential Oil Safety, second ed. Churchill Livingstone Elsevier, United Kingdom, p. 376.

Wojdylo, A., Oszmianski, J., Czemerys, R., 2007. Antioxidant activity and phenolic compounds in 32 selected herbs. Food Chem. 105, 940–949. https://doi.org/10.1016/j.foodchem.2007.04.03.

Figures Legends

Fig. 1. Cell viability assessed by MTT assay of keratinocytes NCTC 2544 treated with *Origanum vulgare* essential oil (OEO) at 0, 3, 5, 7.5, 10, 12, 25, and 50 μg/mL. The values of optical density measured at λ= 550 nm were reported as percentage with respect to the optical density of untreated control cells considered as 100% of cell viability. Each point represents mean ± SD of three separate experiments performed in triplicate.

Fig. 2. Quantification of reactive oxygen species (ROS) levels measured by 2', 7'dichlorodihydrofluorescein diacetate (H_2-DCFDA) assay. The results reported as relative fluorescence units showed a significantly increased ROS production after treatment of NCTC 2544 with IFNγ and histamine. In cells pretreated with *Origanum vulgare* essential oil (OEO) at 25 μg/mL or indomethacin at 10 μM, IFNγ and histamine–induced ROS generation was significantly reduced. Data represent mean ± SD of three separate experiments performed in triplicate. Values are expressed as a percentage of relative fluorescence units with respect to control. *Significant versus untreated control; °significant versus IFNγ and histamine treated; $p \leq 0.05$.

Fig. 3. Determination of 8-OHdG in NCTC 2544 stimulated with INF-γ and H alone or plus 10 μM of indomethacin or 25 μg/mL of OEO measured spectrofluorometrically. The cell density was assayed by the incubation with 4′,6-diamidino-2-phenylindole dihydrochloride (DAPI). Values are expressed as fold change versus untreated control of means ± SD of relative fluorescence units of three separate experiments performed in triplicate. *Significantly different compared to untreated control ($p< 0.05$); °significantly different compared to INF-γ and H-treated samples ($p< 0.05$).

Fig. 4. (A) Microscopic observation of scratch assay of untreated or OEO-treated NCTC 2544 at time T0, 24, 48 and 72 hours after injury. Magnification 10x. (**B**) Graph showing the closure percentage value from T0 to 72 hours after wound. Values are expressed as mean ± SD of three experiments.

*Significant versus untreated control ($p < 0.05$); °Significant versus untreated control at the same time point ($p < 0.05$).

Fig. 5. Determination by RT-PCR (**A**) and Western blot (**B**) of ICAM-1, NOS2, and COX-2 in NCTC 2544 untreated or treated with INF-γ and H alone or plus 10 μM of indomethacin or 25 μg/mL of OEO expressed as $2^{-\Delta\Delta CT} \pm$ SD and as arbitrary densitometric units (A.D.U.) ± SD, respectively. *Significant versus untreated control; °significant versus INF-γ and H only treated; $p \leq 0.05$.

Fig. 6. Determination by RT-PCR and Western blot of MMP-1 in NCTC 2544 untreated or treated with INF-γ and H alone or plus 10 μM of indomethacin or 25 μg/mL of OEO expressed as $2^{-\Delta\Delta CT} \pm$ SD and as arbitrary densitometric units (A.D.U.) ± SD, respectively. *Significant versus untreated control; °significant versus INF-γ and H only treated; $p \leq 0.05$.

Fig. 7. Determination by RT-PCR and Western blot of MMP-12 in NCTC 2544 untreated or treated with INF-γ and H alone or plus 10 μM of indomethacin or 25 μg/mL of OEO expressed as $2^{-\Delta\Delta CT} \pm$ SD and as arbitrary densitometric units (A.D.U.) ± SD, respectively. *Significant versus untreated control; °significant versus INF-γ and H only treated; $p \leq 0.05$.

Fig. 8. Determination by RT-PCR and Western blot of PCNA protein in NCTC 2544 untreated or treated with INF-γ and H alone or plus 10 μM of indomethacin or 25 μg/mL of OEO expressed as $2^{-\Delta\Delta CT} \pm$ SD and as arbitrary densitometric units (A.D.U.) ± SD, respectively. *Significant versus untreated control; °significant versus INF-γ and H only treated; $p \leq 0.05$.

Table 1: List and percentage of identified compounds in *Origanum vulgare* essential oil (OEO)

#[a]	Class/Compound[c]	Oregano %
	Monoterpene hydrocarbons	29,24
924	α-thujene	0.07 ± 0,005
931	α-pinene[b]	1,37 ± 0,0206
947	camphene[b]	0,56 ± 0,0079
974	β-pinene	0,43 ± 0,0090
976	3-Octanone	0,10 ± 0,0025
986	myrcene[b]	0,66 ± 0,0140
993	Octanol<3->	0,05 ± 0
999	Carene<delta-2>	0,06 ± 0,0015
1007	Mentha-1(7),8-diene<*p*->	0,01 ± 0,0006
1027	*p*-cymene[b]	21,54 ± 0,3508
1029	limonene[b]	0,78 ± 0,0444
1031	Eucaliptolo	0,84 ± 0,0229
1037	*o*-cymene	0,04 ± 0,0006
1058	γ-terpinene[b]	2,16 ± 0,0392
	Oxygenated monoterpenes	
1073	Linalool-oxide<cis->	0,03 ± 0,0141
1098	Linalool[b]	4,26 ± 0,0518
1124	Mentha-2en-1-ol<cis-*p*->	0,02 ± 0,0005
1144	Camphor	0,36 ± 0,0556
1158	Isoborneol	0,27 ± 0,1519
1167	borneol[b]	0,90 ± 0,0263
1177	terpinen-4-ol[b]	0,35 ± 0,0070
1243	carvacrol methyl ether[b]	0,16 ± 0,0213
1303	thymol[b]	**25,02 ± 0,2703**
1319	carvacrol[b]	**35,95 ± 0,2263**
1353	α-Terpinyl acetate	0,03 ± 0,0020
1361	Eugenolo	0,11 ± 0,0006
	Sesquiterpenes	0,61
1379	α-copaene[b]	0,03 ± 0,021
1425	β-caryophyllene[b]	1,70 ±
1459	α-humulene[b]	0,24 ± 0,0153
1509	β-bisabolene	0.02 ± 0.0006
1588	caryophyllene oxide	0.18 ± 0.0047
	Others	**0.02 ± 0.001**
976	octen-3-ol	0.21 ± 0.0045

[a] The numbering refers to elution order and values (relative peak area percent) represent averages of 3 determinations.
[b]Co-elution with authentic sample.
[c]Compounds with a % less than 0.1 were not reported.

Table 2: RT-PCR primers list

Target gene	Primers sequence	
iNOS	GTTCTCAAGGCACAGGTCTC	GCAGGTCACTTATGTCACTTATC
ICAM-1	GGCCGGCCAGCTTATACAC	TAGACACTTGAGCTCGGGCA
COX-2	ATCATTCACCAGGCAAATTGC	GGCTTCAGCATAAAGCGTTTG
MMP-1	GGTGATGAAGCAGCCCAG	CAGTAGAATGGGAGAGTC
MMP-12	CCACTGCTTCTGGAGCTCTT	GCGTAGTCAACATCCTCACG
GAPDH	TCAACAGCGACACCCAC	GGGTCTCTCTCTTCCTCTTGTG

Table 3: Antibodies list

Antibody	Code	Dilution	Product
8-OHdG	sc-393870	1:200	Santa Cruz Biotechnology, DBA, Milan, Italy
PCNA	A300-277A-M	1:2000	Bethyl Laboratories, Bologna, Italy
iNOS	sc-651	1:200	Santa Cruz Biotechnology, DBA, Milan, Italy
ICAM-1	sc-51632	1:200	Santa Cruz Biotechnology, DBA, Milan, Italy
COX-2	sc-1745	1:200	Santa Cruz Biotechnology, DBA, Milan, Italy
MMP-1	sc-21731	1:200	Santa Cruz Biotechnology, DBA, Milan, Italy
MMP‐12	sc-390863	1:200	Santa Cruz Biotechnology, DBA, Milan, Italy
β-actin	A-2066	1:20000	Sigma Aldrich, Milan, Italy

Fig. 1

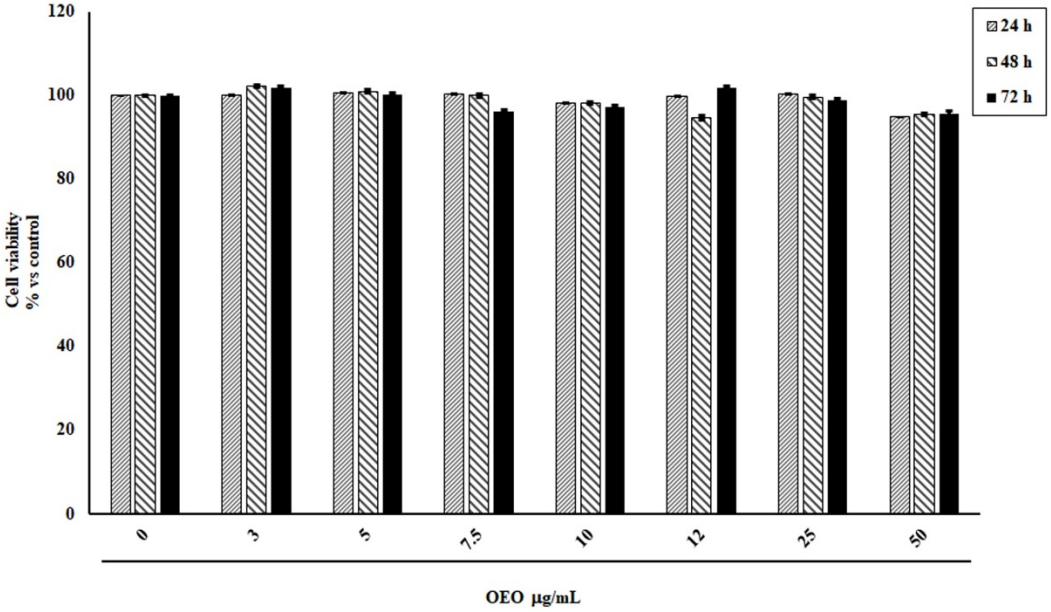
120
100
80
60
40
20
0
Cell viability
% vs control
24 h
48 h
72 h
0
3
5
7.5
10
12
25
50
OEO µg/mL

Fig. 2

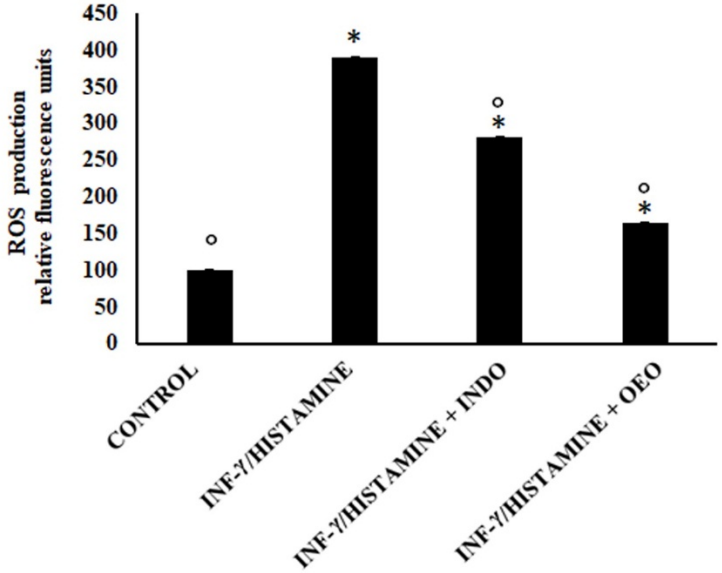
450
400
350
300
250
200
150
100
50
0
ROS production
relative fluorescence units
CONTROL
INF-γ/HISTAMINE
INF-γ/HISTAMINE + INDO
INF-γ/HISTAMINE + OEO

Fig. 3

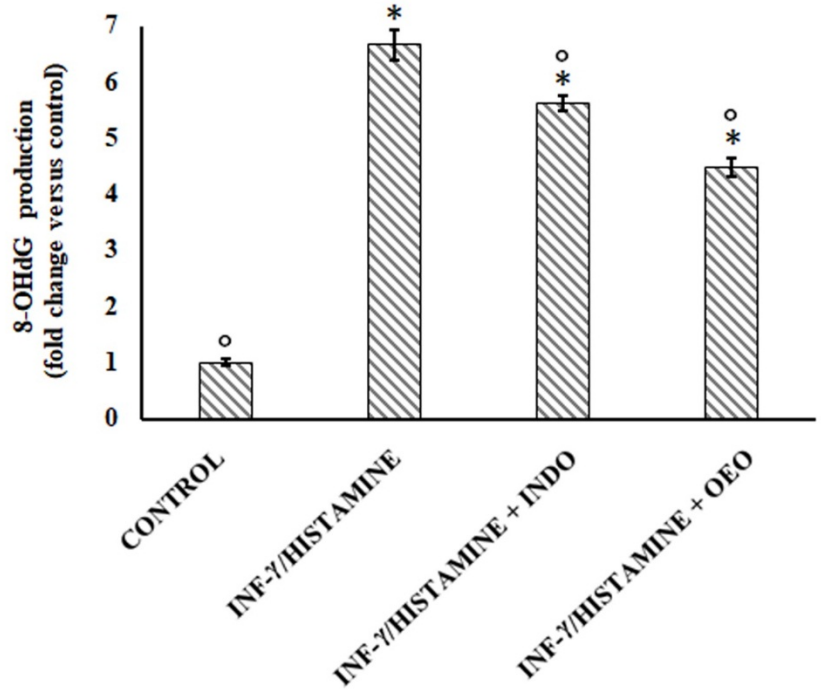
8-OHdG production
(fold change versus control)
0
1
2
3
4
5
6
7
CONTROL
INF-γ/HISTAMINE
INF-γ/HISTAMINE + INDO
INF-γ/HISTAMINE + OEO

Fig. 4

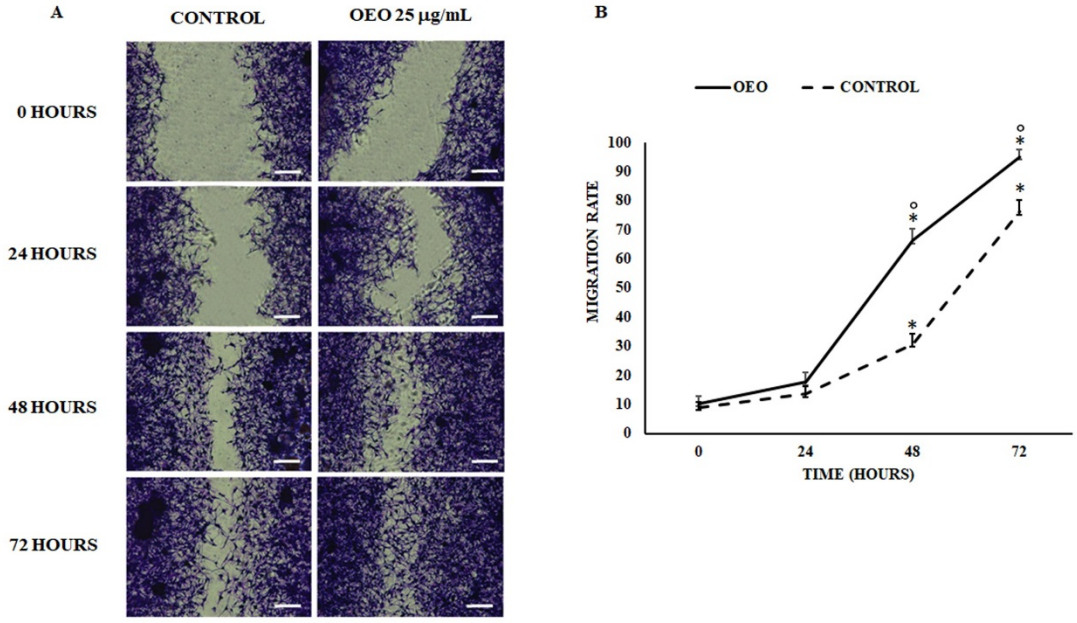
A
CONTROL
OEO 25 µg/mL
0 HOURS
24 HOURS
48 HOURS
72 HOURS
B
OEO
CONTROL
MIGRATION RATE
0
10
20
30
40
50
60
70
80
90
100
0
24
48
72
TIME (HOURS)

Fig. 5

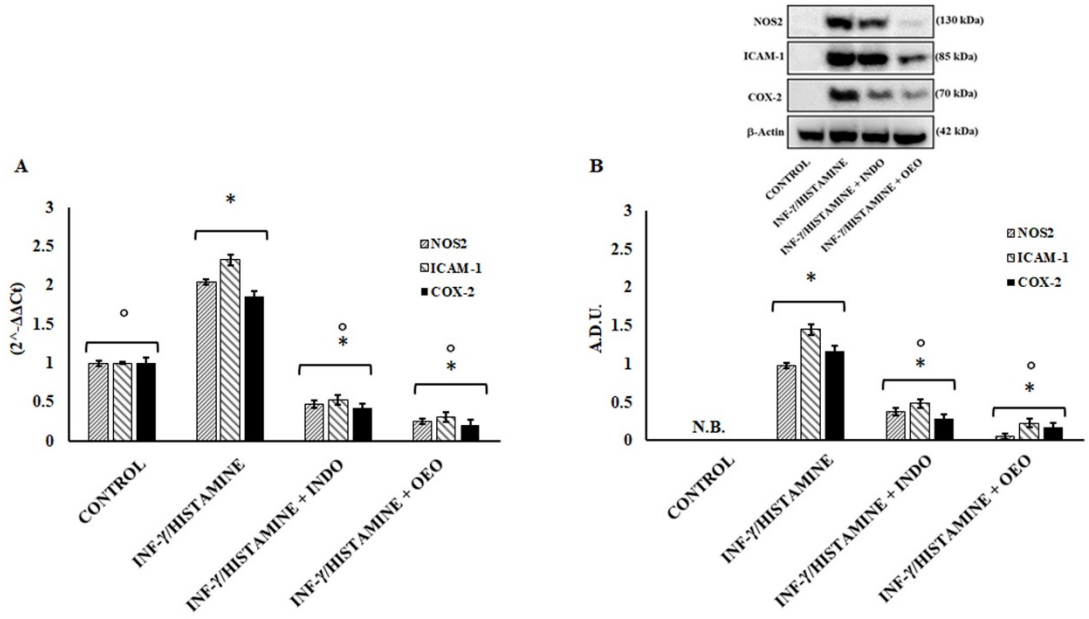
A
(2^-ΔΔCt)
NOS2
ICAM-1
COX-2
CONTROL
INF-γ/HISTAMINE
INF-γ/HISTAMINE + INDO
INF-γ/HISTAMINE + OEO
B
NOS2 (130 kDa)
ICAM-1 (85 kDa)
COX-2 (70 kDa)
β-Actin (42 kDa)
A.D.U.
N.B.

Fig. 6

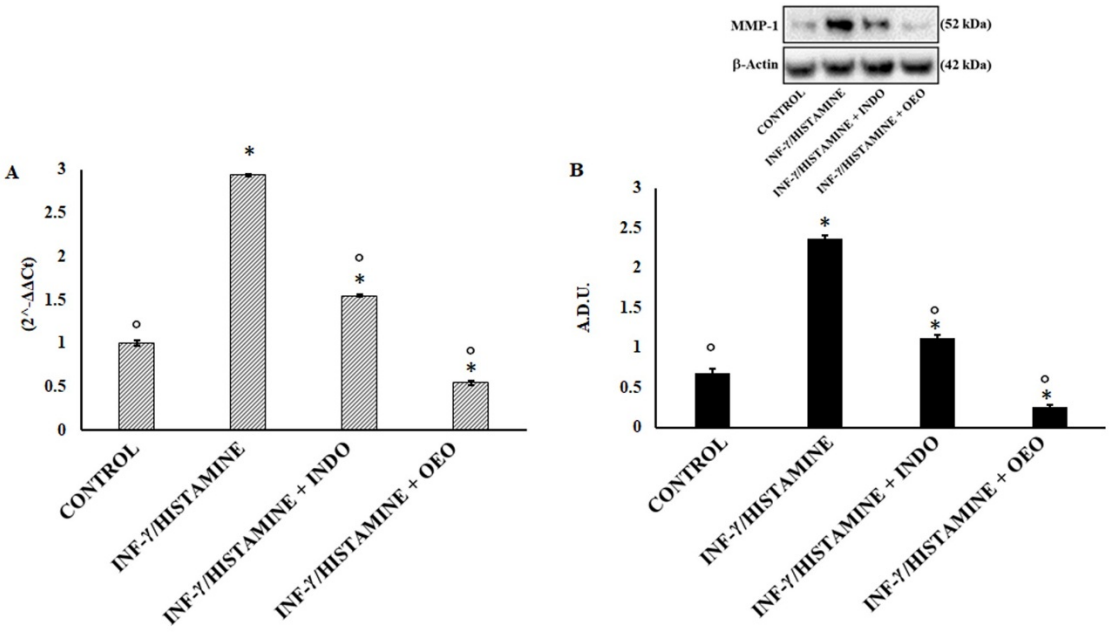
A
(2^-ΔΔCt)
CONTROL
INF-γ/HISTAMINE
INF-γ/HISTAMINE + INDO
INF-γ/HISTAMINE + OEO
B
MMP-1 (52 kDa)
β-Actin (42 kDa)
A.D.U.

Fig. 7

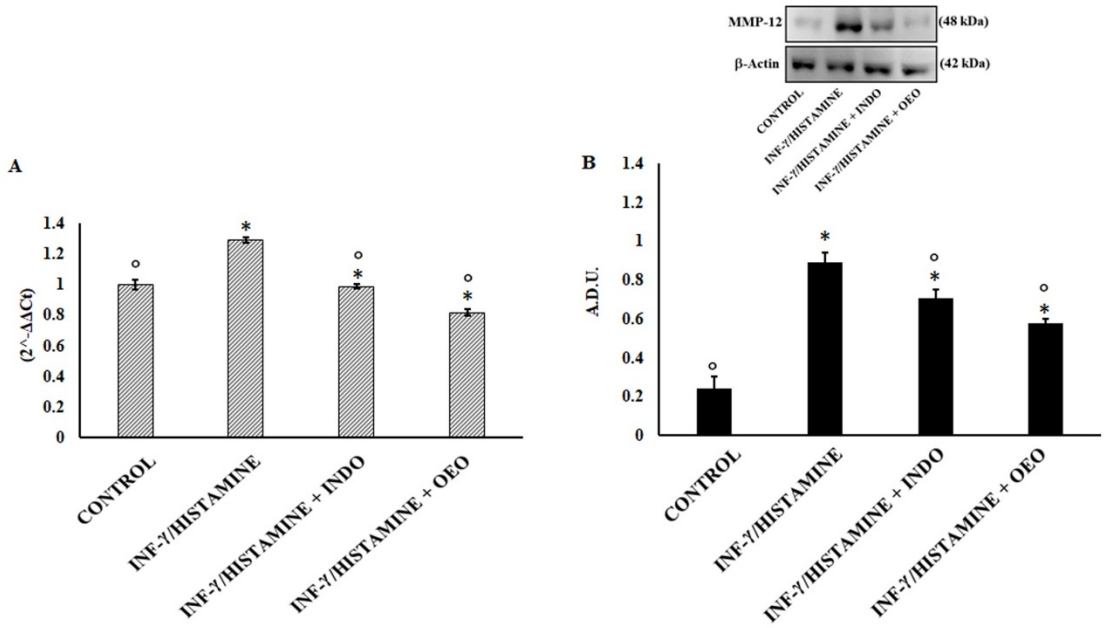
A
(2^-ΔΔCt)
1.4
1.2
1
0.8
0.6
0.4
0.2
0
CONTROL
INF-ɣ/HISTAMINE
INF-ɣ/HISTAMINE + INDO
INF-ɣ/HISTAMINE + OEO
B
MMP-12
(48 kDa)
β-Actin
(42 kDa)
A.D.U.
1.4
1.2
1
0.8
0.6
0.4
0.2
0
CONTROL
INF-ɣ/HISTAMINE
INF-ɣ/HISTAMINE + INDO
INF-ɣ/HISTAMINE + OEO

Fig. 8

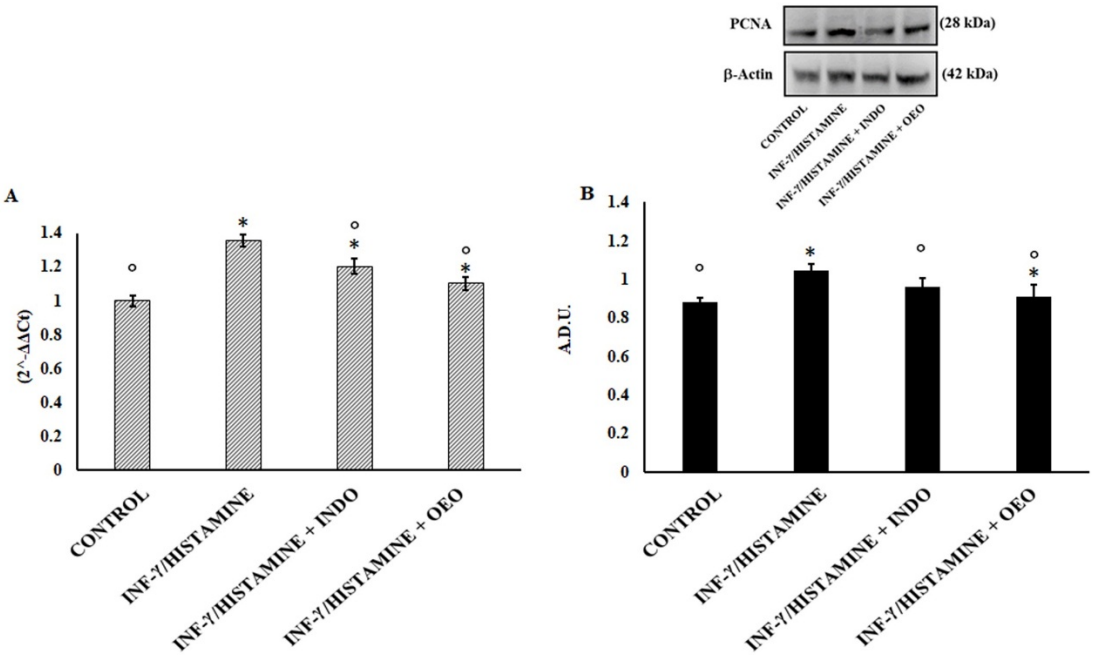
A
(2^-ΔΔCt)
1.4
1.2
1
0.8
0.6
0.4
0.2
0
CONTROL
INF-ɣ/HISTAMINE
INF-ɣ/HISTAMINE + INDO
INF-ɣ/HISTAMINE + OEO
B
PCNA
(28 kDa)
β-Actin
(42 kDa)
A.D.U.
1.4
1.2
1
0.8
0.6
0.4
0.2
0
CONTROL
INF-ɣ/HISTAMINE
INF-ɣ/HISTAMINE + INDO
INF-ɣ/HISTAMINE + OEO